Voltage and Current Response Characteristics of PMU Device by PCI Simulation

Liang Zhang[1], Wei Qiu*[1], He Yin[1]
Department of EECS
[1]University of Tennessee,
Knoxville, USA
{lzhan104, qwei4, hyin8}@utk.edu

Lawrence C Markel[2], DaHan Liao[2],
Ben W McConnell[2], Yilu Liu[1,2]
[2]Oak Ridge National Laboratory, Oak Ridge
Knoxville, USA
{markellc, liaod, mcconnellbw}@ornl.gov, liu@utk.edu

***Abstract*— Phasor Measurement Units (PMUs) are critical for the Wide Area Measurement System (WAMS), especially for real-time grid monitoring, disturbance location, and situation awareness. Once they are damaged, the stable operation of power system will be affected directly and greatly. As new electronic devices in power system, their immunity to electromagnetic pulse (EMP) events needs to be studied. In this paper, an effective impedance measurement scheme is proposed for port impedance measurement of PMU. A non-uniform transmission line model is established to eliminate the impact of fixture in the de-embedding process. Then circuit of pulse current generator is established to generate damping sinusoid and double exponential wave applied to the port. Finally, by using measured impedance as load of the generator, the voltage and current responses of different ports are calculated in the pulsed current injection (PCI) simulation. Results shows the characteristics of port impedance, voltage and current waveforms. The relation between port impedance and the waveforms is discussed.**

***Index Terms*— Phasor Measurement Units (PMU), electromagnetic pulse (EMP), impedance measurement, Pulsed Current Injection (PCI)**

I. Introduction

Phasor Measurement Units (PMUs) are critical for the Wide Area Measurement System (WAMS), especially for real-time grid monitoring, disturbance location, and situation awareness [1]. More than 2000 PMUs units have been deployed in the United States, which is distributed in different nodes of the power grid [2]. Therefore, the reliability of the PMU directly affects the stable operation and control of the power system. The experiences of extreme weather have improved the resilience of the WAMS system [3]. However, few studies have focused on the stability and reliability of PMUs under the Electromagnetic Pulse (EMP), where the EMP is a type of short burst of electromagnetic energy. The EMP can be easily coupled to PMUs through transmission lines and antennas (GPS receiver), thereby damaging the circuit of the equipment. It is urgent and necessary to study the immune response of PMUs under EMP [4].

This work is supported in part by the DOE Grid Modernization Lab Call (GMLC): Project Vulnerability of Power Generation Critical Systems Against Electromagnetic Threats under Agreement #36129, and also in part by CURENT Industry Partnership Program.

Generally, immunity levels of equipment to EMP can be measured by radiative test. But it needs large power impulse source and should put the device under EM environment, so it is not easy to carry out. Instead, pulsed current injection (PCI) test is a good replacement for it and is usually used in conducted immunity test.

This paper aims to study the circuit response of PMU device under EMP by PCI simulation. First, port impedance of PMU is measured by network analyzer and LCR meter. And then pulse current generators are established to output pulse current and voltage according to IEC standard. Finally, by using port impedance as the load and applying pulse voltage, transient response under EMP for typical ports are obtained. Voltage and current waveforms and their cumulative energy are analyzed.

II. Impedance Measurement

Electromagnetic pulses typically comprise a wide frequency range from Hz level to GHz level. The impedance measurement devices should have a wide frequency range. However, most of the measuring instruments can only provide a specific range of frequency. Therefore, three instruments are used together to obtain the actual impedance results in this section.

The evaluation of these three instruments is listed in Fig. 1 and Table I. The LCR meter is one type of commonly used device to measure inductance (L), capacitance (C) and resistance (R) [5]. Network analyzer (NA) is an instrument that measures the network parameters of electrical networks [6].

HP 4395A　　LCR meter　　Planar TR 1300/1

Figure 1. Impedance measurement instruments.

For the LCR meter, the measurement value is discrete data points, which a total of 41 frequency points can be obtained from 40 Hz to 200 kHz. The impedance analyzer HP 4395A and VNA Planar TR1300/1 have more measurement points, which can reach 805 and 16001 points, respectively. This means that they have a higher resolution compared with the LCR meter. LCR meter has a higher measurement range than NA and it is mainly used to supplement the impedance of the low frequency part.

TABLE I

FEATURES OF THREE IMPEDANCE MEASURING INSTRUMENTS

	LCR meter	Imp. Analyzer	VNA
Name	MCR-5200	HP 4395A	Planar TR1300/1
Adapter	-	HP 87512A	N1.1 Calibration Kit
Freq. range	40Hz-200kHz	10Hz-500MHz	300kHz-1.3GHz
Imp. range	0.1mΩ−99.99MΩ	< 40kΩ	<100kΩ
Accuracy	> 0.1%	3%-10%	0.5%-3%

To ensure consistent results, output voltages of the three instruments are all set to a relatively low value, 0.1V. Corresponding output power is -7 dBm. The impedance measurement setup is shown in Fig. 2. Calibration is done at the end of the cable and a fixture is needed to connect the device under test (DUT, namely PMU) and the cable.

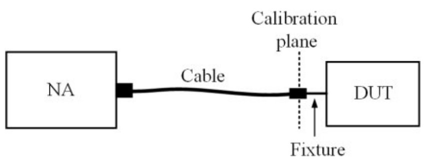

Figure 2. Impedance measurement using network analyzer.

The measurement results contain the impedance from both PMU port and the fixture. This may bring some errors for measuring relatively large or small impedance values. Therefore, the de-embedding process is necessary to eliminate the influence of the fixture [7].

III. DE-EMBEDDING PROCESS

To obtain the actual impedance of PMU ports, the commonly used method is the open-short or short-open de-embedding method [8]. It has an effective effect in the low-frequency part. However, it should be noted that the wires among the ground and signal also have the resistance and inductance in the short pattern, leading to bias at high frequencies. In this section, a de-embedding method is established to eliminate the impact of fixtures. It is based on the non-uniform transmission line model.

By trying and fitting, a seven-stage cascade of the transmission line model is shown in Fig. 3. Left side is connected to cable and right side is connected to DUT. Resistance, inductance, and capacitance are the three main parameters. To obtain these parameters, the total parallel capacitance and serial inductance are estimated based on measured open and short circuit impedance.

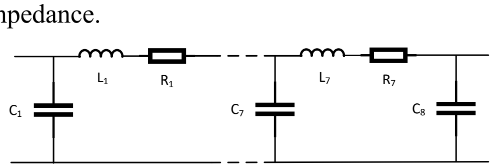

Figure 3. Non-uniform transmission line model in de-embedding of fixture.

Basically, wire distance d_f, will affects both the capacitance and inductance of the fixture. Impedance of several conditions shown in Fig.4 are measured.

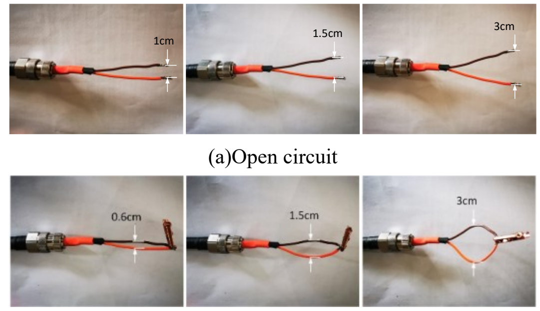

(a)Open circuit

(b)Short circuit

Figure 4. Open and short Impedance measurement of different d_f.

The C_t and L_t with distances $d_f \in \{0.6cm{-}3cm\}$ are calculated, as shown in Fig. 5. The capacitance is changing with the distance between two wires. The mean value can be obtained and is located in 3.4 pF to 3.8 pF. Considering that the distance between two wires is usually about 2 cm, an average capacitance C_t is set to 3.7pF. Meanwhile, the total serial inductance L_t is distributed in 60 nH to 100 nH when f is lower than 100 MHz. The average value is set to 80 nH. The resistance of the non-uniform transmission line model can also be obtained from the short circuit impedance.

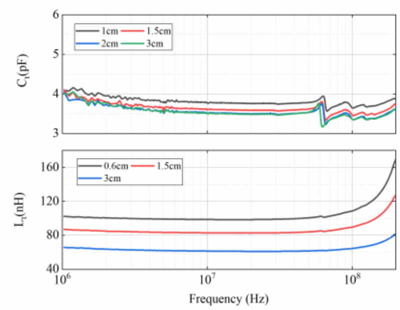

Figure 5. Calculated total capacitance and inductance C_t and L_t in different d_f.

Based on the resonance points, trial and errors, the estimated C_i and L_i for each stage are estimated and listed in Table II.

Table II

DISTRIBUTION OF CAPACITORS AND INDUCTORS IN THE DE-EMBEDDING MODEL

Number	1	2	3	4	5	6	7	8
C_i(pF)	1.8	0.7	0.5	0.25	0.15	0.1	0.09	0.07
L_i(nH)	7.4	9.8	12.3	12.3	12.3	12.3	12.3	--

Fig.6 shows the measured and calculated open circuit impedance of fixture. They are consistent both in the amplitude and phase. This is a verification for transmission line model of the fixture.

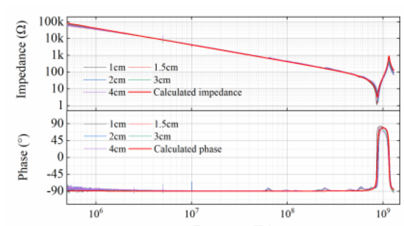

Figure 6. Measured and calculated open circuit impedance of fixture.

After de-embedding, the measured impedance needs to be further integrated since there are three sets of measurement results. This is realized by interpolation and curve fitting. An example of port impedance measurement results and combination are shown in Fig.7. Fig.7(a) is the port impedance measured by three instruments. In the low frequency part, values have exceeded the measurement range of NA. So LCR meter measurement provides the correct values. Fig.7(b) shows the integrated results.

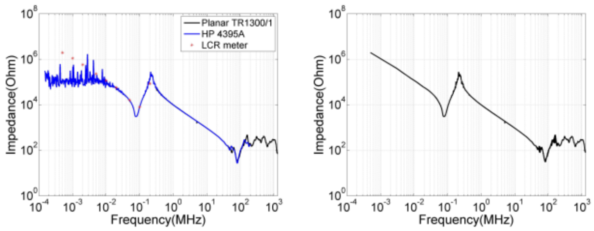

(a)Measurement results (b)Integrated results

Figure 7. Impedance measurement results and integrated results.

IV. Pulsed Current Injection Simulation

The simplified circuit diagram of PCI is shown in Fig. 8 based on IEC 61000-4-25 [9]. Although there are twelve immunity test levels, basically two types of output waveforms are adopted, namely damped sinusoids for lower EC1-EC6 level and double exponential waveform for higher six levels [9-10].

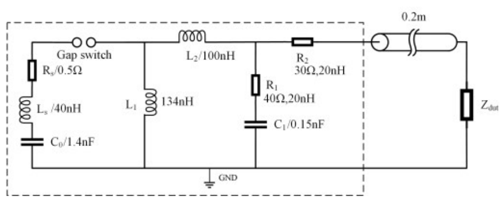

(a) EC5 level

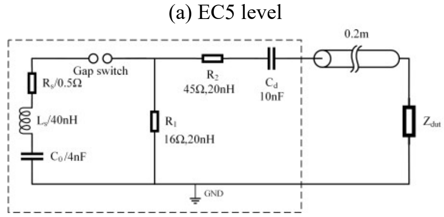

(b) EC8 level

Figure 8. The circuit diagram of PCI test.

Here EC5 level and EC8 level are simulated and circuit in the dash box represents the pulse current generator. Parameters shown in the figure ensure that the output waveforms meet the requirements of IEC standard. Output of generator is connected to impedance Z_{dut} through a 50 Ω coaxial cable. Z_{dut} represents the measured port impedance of PMUs. When gap switch is triggered, a pulse voltage is applied to the circuit. The voltage and current waveforms on the load are calculated in frequency domain, and then converted to time domain.

For EC5 level, there are three oscillation frequencies: 3MHz, 10MHz and 30MHz. 10MHz waveform is illustrated and the normalized waveforms are shown in Fig.9(a) for typical load of 0.1Ω, 50 Ω and 1000 Ω. With main capacitor charged to 2.3 kV, short current is 40 A and open voltage is 2000 V. Similarly, normalized waveforms of EC8 level are shown in Fig.9(b). With main capacitor charged to 9.05 kV, short current is 160 A and open voltage is 8 kV. All parameters meet the requirements of IEC standard.

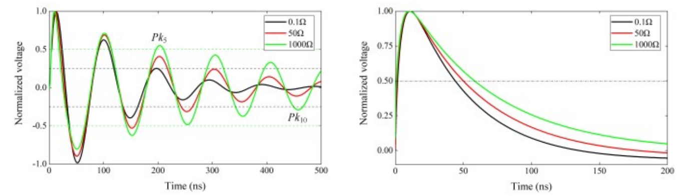

(a) EC5 level (b) EC8 level

Figure 9. The normalized output voltage waveforms of the generator.

V. Experiment Results and Discussions

This section shows the impedance measurement results of PMU and PCI simulation results.

A. *Impedance measurement results of PMU*

Fig.10 shows the PMU to be measured. It is a commonly used type designed by University of Tennessee, Knoxville (UTK).

Figure 10. The measured PMU and ports.

All instruments are warmed up for one hour before measurement. Here GPS antenna, RJ-45 ethernet and AC power ports are selected to be analyzed. There are 8 wires inside ethernet cable and one pair data transmission lines are selected to show here.

As there are common mode and differential mode disturbance, wire-ground and wire-wire impedance are both measured. Results are shown in Fig.11.

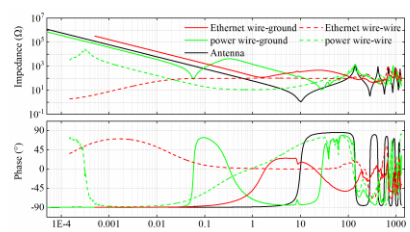

Figure 11. Measured port impedance of UTK PMU.

Different port has different characteristics. For antenna port, impedance is capacitive at low frequency part. Then it decreases to about 1 Ω and oscillates at high frequency part. For ethernet port, wire-ground impedance is also capacitive and has large values at low frequency part. But it is still more than 100 Ω when frequency is higher than 1 MHz. Wire-wire impedance is low at low frequency, and maintain resistive 100 Ω up to 100 MHz. For power port, wire-ground impedance is also large but is only 10 Ω at 30 MHz. Wire-wire impedance is much smaller. The value is about 10 Ω up to 10 MHz and then increase a little with the increase of frequency.

B. Results of pulsed current injection simulation

Based on the circuit of PCI simulation and measured port impedance, voltage and current response for the selected ports can be calculated. Waveforms of voltage and current under EC5 and EC8 are shown in Fig.12 and Fig.13.

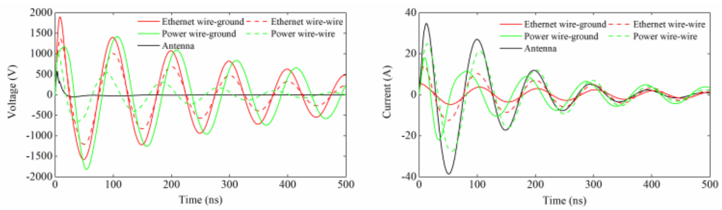

(a) Voltage waveforms (b) Current waveforms

Figure 12. Voltage and current waveforms for different ports under EC5.

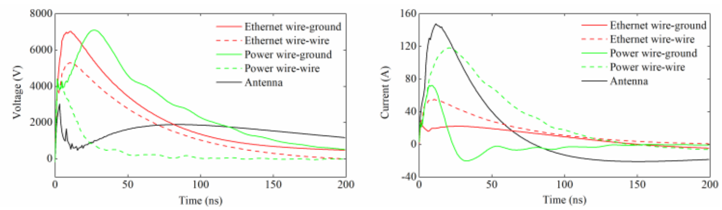

(a) Voltage waveforms (b) Current waveforms

Figure 13. Voltage and current waveforms for different ports under EC5.

It can be seen that higher voltage always come out with lower current, or vice versa. For antenna port, as its low port impedance, current is close to 40 A and 160 A, and voltage is 500 V and 3000 V under EC5 and EC8 respectively. For ethernet port, wire-ground impedance is large, so voltage is high. It is about 2000 V under EC5 and 7000 V under EC8. Corresponding current is small. Smaller wire-wire impedance brings relatively lower voltage and higher current. For power port, voltage and current are about half of open voltage and short current under EC5. This is because the impedance near 10 MHz is about 50 Ω. But under EC8, voltage of wire-ground is much higher than that of wire-wire, show as the green curves in Fig.13(a).

As voltage of EC8 has a large frequency range of components, we need to analyze the port impedance over a larger frequency range. This can be done from the view of cumulative energy aspect. Cumulative energy percentage for voltage and current are shown in Fig.14.

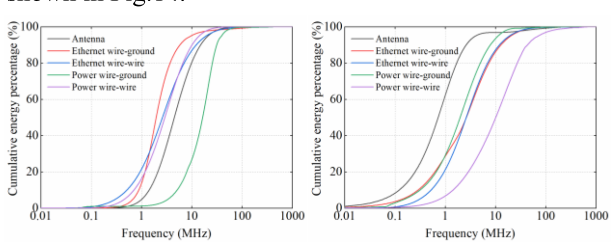

(a) Voltage (b) Current

Figure 14. Cumulative energy percentage for voltage and current under EC8.

Energy is concentrated in different frequency range for different port. If consider 90% of energy distribution, frequency can go down to 0.3 MHz and 0.06 MHz for voltage and current, respectively. And it can go up to 39 MHz and 71 MHz. It also should be noted that 39 MHz comes from power wire-ground in Fig.14(a), but 71 MHz comes from power wire-wire in Fig.14(b). This difference is assumed to be the results of impedance characteristics. More measurements and analysis should be carried out for various ports.

VI. Conclusion

To explore the immunity of PMU device in power system under EMP, this paper proposes an impedance measurement scheme based on three instruments. Then, the non-uniform transmission line model is established to eliminate the effect of the fixture. After the de-embedding, all the measured impedance are integrated, and they show the characteristics of different ports of PMU. Two pulse current generators are designed to generate damping sinusoid and double exponential waveforms. By using port impedance as load, pulsed current injection is further conducted to estimate the voltage and current response of PMU. Voltage and current waveforms are analyzed under EC5 and EC8. Their relation with impedance is revealed with the help of cumulative energy percentage.

Future work will focus on the experimental verification to explore the degree of damage to different ports of PMU and failure probability.

References

[1] B. Singh, N. K. Sharma, A. N. Tiwari, K. S. Verma, and S. N. Singh, “Applications of phasor measurement units (PMUs) in electric power system networks incorporated with FACTS controllers,” International Journal of Engineering, Science and Technology, vol.3, no.3, 2011.

[2] A. G. Phadke and T. Bi, "Phasor measurement units, WAMS, and their applications in protection and control of power systems," in Journal of Modern Power Systems and Clean Energy, vol. 6, no. 4, pp. 619-629, July 2018.

[3] M. Panteli, D. N. Trakas, P. Mancarella and N. D. Hatziargyriou, "Boosting the Power Grid Resilience to Extreme Weather Events Using Defensive Islanding," in IEEE Transactions on Smart Grid, vol. 7, no. 6, pp. 2913-2922, Nov. 2016.

[4] E. Savage, J. Gilbert, and W. Radasky, “The Early-Time (E1) HighAltitude Electromagnetic Pulse (HEMP) and Its Impact on the U.S. Power Grid ,” in Metatech Corporation, Goleta, CA, USA, Meta-R-320, 2010.

[5] R. Malari, P. Mostarac, G. Petrovi, and J. Havelka, “Method for nonlinear fitting and impedance analysis with lcr meter,” in 2016 MIXDES 23rd International Conference Mixed Design of Integrated Circuits and Systems, 2016, pp. 410–414.

[6] K. D. Palmer, and M. W. van Rooyen, “Simple broadband measurements of balanced loads using a network analyzer,” IEEE transactions on instrumentation and measurement, vol.55, no.1, pp.266-272, Jan. 2006.

[7] A. M. Mangan, S. P. Voinigescu, Ming-Ta Yang, and M. Tazlauanu, “De-embedding transmission line measurements for accurate modeling of ic designs,” IEEE Transactions on Electron Devices, vol. 53, no. 2, pp. 235–241, 2006.

[8] I. M. Kang, S. J. Jung, T. H. Choi, J. H. Jung, C. Chung, H. S. Kim, H. OH, H. W. Lee, G. Jo, Y. K. Kim, H. G. Kim, and K. M. Choi, “Five-step (pad–pad short–pad open–short–open) de-embedding method and its verification,” IEEE Electron Device Letters, vol.30, no.4, pp.398-400, Feb. 2009.

[9] IEC:61000-4-25, “Electromagnetic compatibility (EMC), part 4-25: Testing and measurement techniques - HEMP immunity test methods for equipment and systems”, 2019.

[10] IEC:61000-2-10, “Electromagnetic compatibility (EMC) - part 2-10: Environment - description of HEMP environment - conducted disturbance”, 1998.